Journal of Renewable Materials

Tech Science Press

DOI: 10.32604/jrm.2021.016418

ARTICLE

Improvement in the Performance of the Polylactic Acid Composites by Using Deep Eutectic Solvent Treated Pulp Fiber

Lei Tan, Liangxian Liu, Chaodong Liu and Weihong Wang*

Key Laboratory of Bio-Based Material Science and Technology (Ministry of Education), Material Science and Engineering College, Northeast Forestry University, Harbin, 150040, China

*Corresponding Author: Weihong Wang. Email: weihongwang2001@nefu.edu.cn

Received: 04 March 2021 Accepted: 15 April 2021

ABSTRACT

As the most favorable alternative to petroleum-based polymers, polylactic acid (PLA) which is the most promising degradable polymer has attracted increasing attention. However, the addition of cellulose to improve its strength often results in a reduction in its toughness. In this work, microscale cellulose is first prepared from pulp fibers by using a deep eutectic solvent, and then is used as the reinforcement of PLA. A microcrystalline cellulose (MCC)/PLA sheet with uniform texture is obtained by the solution mixing, melt blending, hot-pressing and cold-pressing process. The effects of MCC on the crystallization, thermal stability and mechanical properties of the PLA matrix were studied. Upon the addition of 1% cellulose fiber, the tensile strength of MCC/PLA composite sheet increased by 27%, and the elongation at break did not shown an evident decrease. The strength enhancement mechanism was elucidated using scanning electron microscopy, differential scanning calorimetry, and dynamic thermomechanical analysis. The energy dissipation during the deformation process and the compatibility of AMCC and rougher surface of MCC play important role in the strength enhancement. Additionally, UV spectroscopy showed that the composite material absorbed some ultraviolet light. Our results show that the combined use of a deep eutectic solvent and solution mixing is an effective approach for improving the strength of PLA while maintaining its toughness.

KEYWORDS

Polylactic acid; microcrystalline cellulose; deep eutectic solvent; mechanical properties

1 Introduction

With the increasing emergence and importance of environmental problems, various measures for environmental protection have been proposed such as strict restrictions on the use of plastics. Polylactic acid is the currently most widely commercially used degradable biomass polymer and is expected to become a common substitute for petroleum-based non-degradable polymers. It has been used in electronic parts [1], engineering plastics [2], 3D printing material [3], agricultural mulch films [4], packaging materials [5], and automotive interiors [6] due to its excellent renewability, biodegradability, biocompatibility, and non-toxicity [7]. However, polylactic acid shows the disadvantages of poor roughness and low crystallization rate that give rise to the loss of mechanical properties and narrow operational temperature range [8,9].

To overcome these shortcomings, the addition of cellulose to polylactic acid has been investigated in recent research. As the world's most abundant renewable material, cellulose is widely found in the cell walls of biomass such as bamboo, wood, cotton, hemp and crop straws. It has the characteristics of low cost, high specific strength, and good biocompatibility [10–12]. Some progress has been made in the addition of cellulose to the polylactic acid matrix [13–15], with the obtained composites divided into the categories of large-scale diameter and micro-nano-scale composites according to the size of the cellulose. For the large-scale diameter composites, the use of fibers that are visible to the naked eye is preferred in a composite structure or blend using fibers from sources such as cotton [16,17], hemp [18,19], bamboo [20], wood [21] and other debris. Micro-nano diameter composites are obtained by the combination of the polymer with the fibers mainly transformed from cellulose raw material into the micro-nano scale by physical or chemical means [22–24]. Usually, the large-scale diameter composites are less expensive but the performance of the composite material is somewhat unsatisfactory. By contrast, it has been shown that the addition of micro-nano fibers to polylactic acid not only can improve its mechanical properties but also its crystallization performance [25,26].

The improvement of the performance of polylactic acid by the addition of micro-nano fibers has been reported in previous studies [27,28]. However, the practical use of the micro-nano-cellulose composites has been restricted by the difficulties encountered in the production of micro/nano cellulose. For example, the preparation of micro/nano cellulose by the commonly used TEMPO oxidation or sulfate methods involves the use of sodium hypochlorite and leads to the generation of harmful gases such as hydrogen chloride and chlorine gases. Thus, micro/nano-cellulose production is not environmentally friendly. Additionally, due to its easy agglomeration during blending with polylactic acid, an uneven distribution of cellulose in the composite is obtained. This leads to the decrease in the performance of the resulting composite material, such as greater brittleness and lower strength. Wang et al. [29] prepared the polylactic acid/polyaniline/nanocrystalline cellulose nanocomposite film by the solution casting method. It was found that the addition of cellulose increases the strength and modulus by 38.1% and 89.1%, respectively, but the elongation at break is reduced by 27.3%. Zhang et al. [30] blended MCC with PLA and activated biochar, and the obtained composite material showed increased strength; however, this increase was accompanied by an even greater reduction in the toughness.

In recent years, attractive simple and green methods for the preparation of micro/nano cellulose fibers have been developed. Reports in the literature [31,32] show that the use of a deep eutectic solvent (DES) is an effective approach for the preparation of micro-nano cellulose fibers. DESs are two-component or three-component eutectic mixtures composed of hydrogen bond acceptors (such as quaternary ammonium salts) and hydrogen bond donors (such as amides, carboxylic acids, and polyols) in a certain stoichiometric ratio. The freezing point of a DES is significantly lower than the melting point of each component of the pure substance, and it usually displays the properties of a liquid solvent [33]. By using a DES, nano-cellulose can be prepared rapidly, efficiently and at low cost in a simple, green and pollution-free process. Commonly used eutectic systems are combinations of hydrogen bond donor compounds and organic salts, such as the oxalic acid dihydrate/choline chloride system (melting point 80°C), and the urea/choline chloride system (melting point 90°C), that due to their low melting point enable easy preparation of nano-cellulose with simple processing conditions [34]. However, acidic systems show slightly stronger processing capability and enable the efficient extraction of the lignin in the wood fiber to obtain cellulose with higher purity. Additionally, acidic systems can also swell the cellulose, breaking the links between the component molecular chains and the fibrillation barriers. In an alternative approach to improving the uniformity of cellulose distribution in plastic matrix, the solution mixing method [35,36] has been studied. A part of the plastic is first dissolved in the solvent, and then mixed with fibers. Then, after the removal of the solvent, the mixture was further mixed with the remaining matrix plastic.

In the present study, the deep eutectic solvent and solution mixing methods were combined in order to improve the performance of the cellulose/polylactic acid composite and specifically to obtain a favorable balance of the tensile strength and toughness of polylactic acid. Pulp fibers were first reduced to the micro scale using a deep eutectic solvent and then were distributed in the polylactic acid matrix by the solution mixing method. To further improve the compatibility between the cellulose and polylactic acid matrix, a coupling agent modification was performed for the obtained microcellulose fibers. The results of present study suggest that the combination of the deep eutectic solvent and solution mixing methods enables preparation of bio-composites with improved performance.

2 Experimental and Methods

2.1 Materials

The poplar pulp board treated with sulfate was selected as the raw material. The polylactic acid (PLA, 2003D, D-lactic acid: 1.4%, L-lactic acid: 98.6%, granular, density 1.24 g/cm^3, melt index 5.0–7.0 g/10 min) has a digital mean molecular weight (Mn) and a mean weight (MW) of ∼150,000 and ∼200,000 Da, respectively, and was provided by Nature works (USA). Analytically pure 3-aminopropyl triethoxysilane (APS) was provided by Shanghai McLean Biochemical Technology Co., China. Analytical pure methylene dichloride was provided by Tianjin Fuyu Fine Chemical Co., China. Analytical pure oxalic acid dihydrate was provided by Tianda Chemical Reagent Factory, Tianjin, China. Analytical pure choline chloride was provided by Tianjin Guangfu Institute of Fine Chemicals, China.

2.2 Reduction of Pulp Fiber to Microcellulose with Deep Eutectic Solvent (DES)

The pulp board was cut into small pieces and broken into flocculent fibers using a shredder. The flocculent cellulose fibers were oven-dried at 103°C for 8 h. Choline chloride and oxalic acid dihydrate were mixed in the molar ratio of 1:1 in a flask at 90°C for 2 h and a clear DES was obtained. The dry pulp fibers were added to the flask containing DES. After continuously stirring at 80°C for 2 h, the mixture solution was rinsed with deionized water four times to remove DES and the cellulose aqueous solution was adjusted to 0.5 wt%. Next, the solution was treated with an ultrasonic plant grinder (Scientz-18 N, power: 800 W, Ningbo, China) for 30 min. Then, the ultrasonic cellulose fibers were freeze-dried, and then reduced by a grinder (FZ102, Tianjin, China) to obtain microcellulose powder (MCC).

2.3 Modification of Microcellulose with APS

The APS coupling agent was first mixed with an ethanol/water (ratio of 90/10) solution at the concentration of 10% (based on the total mass of ethanol/water mixture). The obtained microcellulose powder was added to water to prepare a cellulose suspension. Then, the ethanol/water/APS mixture solution was added to the microcellulose aqueous suspension. After stirring at room temperature for 2 h, the APS/ethanol/water/cellulose mixture was heated at reflux at 90°C for 3 h. After the solution was cooled to room temperature, ethanol and APS were removed with deionized water rinsing and vacuum filtration. The APS-modified cellulose aqueous solution was treated with the ultrasonic plant grinder for 30 min, and then was freeze-dried and grinded to the micro scale to obtain modified cellulose (AMCC).

2.4 Prepare Cellulose-Reinforced PLA Composite Sheet

The prepared MCC or AMCC was added to dichloromethane. After even mixing, some of PLA particles of the formulation were added. The mixture was continuously stirred at room temperature for 2 h to dissolve the PLA particles. After the cellulose/PLA mixture solution was obtained, the dichloromethane was evaporated and recycled in a fume hood. The cellulose/PLA mixture was oven dried for 8 h and then broken into powder. The obtained dry powder was continuously mixed with the remaining PLA and melt-compounded in a torque rheometer (Polylab OS, Thermo Fisher Scientific, China). The melt blend of cellulose/PLA was first pre-pressed in a frame at 180°C for 3 min under 0 MPa and then hot-pressed for

5 min under a pressure of 5 MPa at the same temperature. After cooling to room temperature, a sheet with the dimensions of 10 cm × 10 cm × 0.4 mm was obtained. The ratio of PLA to the modified or unmodified cellulose was 100/0.5, 100/1, and 100/2.

3 Characterization

3.1 Fourier Transform Infrared Spectroscopy

A Fourier transform infrared spectrometer (FTIR, Nicolet 6700, Thermo Fisher Scientific Instruments Co., USA) with an attenuated total reflection accessory was used to measure the chemical properties of MFC powders. The sample was placed on the sample table and the pressure tower was adjusted to a suitable position for testing. The scanning range was 400 cm^{-1} to 4000 cm^{-1}. The resolution was 4 cm^{-1} and the number of scans was 32.

3.2 X-ray Diffraction

The crystal structure and crystallinity of the MFC, AMFC and original pulp fibers were examined using an X-ray diffractometer (XRD, D/MAX 2200, Rigaku Instruments Co., Japan). A copper target was used for the experiment, the X-ray wavelength was 0.154 nm, the scanning angle range was 5–45°, the scanning speed was 5°/min, the test step was 0.006°, the tube current was 30 mA, and the tube voltage was 40 KV. The relative crystallinity of the sample was calculated according to

$$CrI = \frac{I_{200} - I_{am}}{I_{200}} \times 100 \quad (1)$$

where CrI is the relative crystallinity (%), I_{200} is the maximum intensity of the absorption diffraction peak of the 002 crystal plane, and I_{am} is the minimum peak intensity between the diffraction absorption peaks of the 101 and the 002 crystal planes [37].

3.3 Scanning Electron Microscopy

The samples of PLA and its reinforced composites were first gold-sprayed in the vacuum coating machine and then an scanning electron microscope (SEM, EM-30 Plus, Korea Coolsham Company, Korea) was used to observe their surface and tensile cross-section. The scanning voltage was 10 kV.

3.4 Tensile Property Test

A universal testing machine (CMT-5504, Shenzhen Xinsansi Material Testing Co., China) was used to measure the tensile properties of PLA and the cellulose-reinforced PLA composite. According to the reference standard GB/T1040.2-2006 (Determination of plastic tensile properties), the test piece was cut into a dumbbell-shape. The length of sample was 75 mm, the narrow part width was 5 mm, the gauge length was 25 mm, and the tensile speed was 5 mm/min. Eight specimens were used for testing in each group.

3.5 Differential Scanning Calorimetry

The crystallinity of PLA and its reinforced composites was analyzed by differential scanning calorimetry (DSC, Q20, TA Company, USA). The samples (3–5 mg) were first heated from 30°C to 200°C at a rate of 10 °C/min and were held at 200°C for 5 min. Then, temperature was rapidly reduced to 30°C and held for 5 min. The samples were then again heated to 200°C at a rate of 10 °C/min.

3.6 Thermogravimetric Test

Thermogravimetric (TG) analysis of the MFC/PLA composites was carried out using a thermogravimetric analyzer (Q50, TA Company, USA). The test temperature ranged from 30°C to 700°C,

and the heating rate was 10 °C/min. To prevent the oxidative degradation of the sample, the test was performed in nitrogen atmosphere at a nitrogen flow rate of 40 ml/min.

3.7 Dynamic Thermomechanical Analysis

The thermo-tensile properties of PLA and MFC/PLA composites materials were tested using a dynamic thermomechanical analyzer (DMA, Q800, TA Company, USA). The test sample was a long strip with the dimensions of 30 mm × 10 mm × 0.4 mm. The testing temperature range was 25°C–120°C, the heating rate was 3 °C/min, the frequency was 1 Hz, and the amplitude was 15 μm.

3.8 Transmittance Test

The transmittance of the MFC/PLA composite sheet was measured using a UV-visible photometer (Cary 100, Agilent, USA). The UV-visible light wavelengths were scanned in the range of 190–900 nm at an interval of 1 nm.

4 Results and Discussion

4.1 Characteristics of MCC and APS-Modified MCC

To explore the microscopic changes of the cellulose before and after the APS modification, scanning electron microscopy was performed **(**Figs. 1a–1c**)**. After undergoing the DES treatment, the pulp fiber cellulose morphology changed from long fiber filaments to rod (Fig. 1b**)**. This is because together with the ultrasonication treatment, DES breaks the links between the component molecular chains and fibrillation barriers through wetting and swelling. Image analysis software was used to obtain the distribution of the cellulose aspect ratio as shown in Fig. 2. It is observed from the figure that the peak aspect ratio prior to the modification was 4, but other aspect ratios values were also observed. After modification, the peak aspect ratio of cellulose was still 4, and the distribution was more concentrated. It is also observed that the surface of the fiber treated with the eutectic reagent is rough, but becomes relatively smooth after the modification by APS. This may be due to the adhesion of APS to the surface of MCC that achieves the same polarity as the polylactic acid matrix through hydrogen bonding with the surface and is expected to improve the compatibility between the cellulose and the PLA matrix.

Fig. 1d shows the change in the functional groups of MCC after APS modification. The characteristic peaks of cellulose are detected in both MCC and modified MCC spectra at 1640 cm^{-1} and 1430 cm^{-1} corresponding to the hydroxyl (-OH) and the vibration of the alkyl group ($-CH_2$), respectively. After APS modification, these two peaks become weak and a new peak appears at 1277 cm^{-1} corresponding to the C-Si-O bond. This is attributed to the reaction between cellulose and APS as shown in Scheme 1, indicating the successful modification of cellulose. Because of the modification by APS, the hydroxyl groups on the cellulose chain were reduced, decreasing cellulose agglomeration. The weakened cellulose interactions and the generated C-Si-O are expected to enhance the bonding between the cellulose and the PLA matrix.

Fig. 1e shows the XRD patterns of cellulose used to examine its crystallinity. Before and after the APS treatment, the same characteristic peaks representing the type I crystal structure were observed at 14.7°, 16.8° and 22.3°. The crystallinity of raw pulp fiber was calculated as 51.32%. After eutectic treatment, the crystallinity is increased to 62.82%, and rose monotonically to 65.45% after APS modification. It has been pointed out in a previous study that ultrasonication cannot increase the cellulose crystallinity [12]. Rather, the increase in the cellulose crystallinity arises mainly from the effect of the eutectic agent on the amorphous region of the cellulose chain. These treatments are beneficial for improving the reinforcement effect.

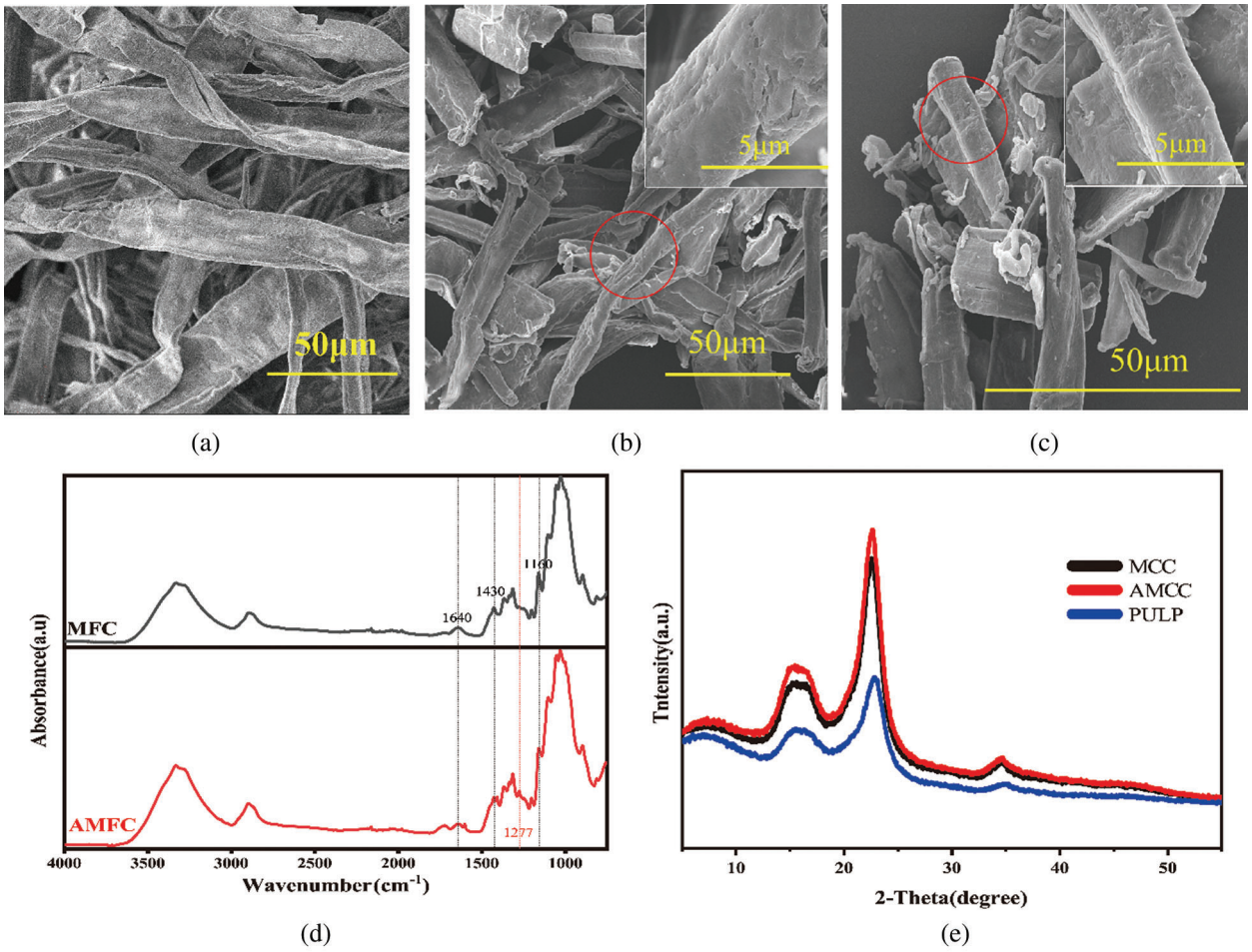

Figure 1: SEM images of (a) pulp fiber (b) MCC and (c) AMCC; (d) FTIR spectra of APS-modified MFC (AMCC) and unmodified MCC; (e) XRD of MCC, AMCC and pulp fiber (PULP)

4.2 Tensile Properties of Cellulose-Reinforced PLA

Fig. 3 shows the results of the elongation at break, tensile strength, and tensile modulus of PLA and its reinforced composites. After the addition of 0.5% MCC to PLA, the tensile strength increased from 56 MPa for PLA to 67 MPa for the MCC/PLA composite, corresponding to an increase of approximately 20%. Meanwhile, the tensile strain at break changes negligibly. This combination of properties is superior to most materials reported in the literature for which the improvement in the strength was accompanied by the decreased in the elongation at break [29,30]. The DES treatment can retain the toughness and provide tensile enhancement to the obtained MCC/PLA composite. With the increase in the fiber content from 0.5% to 1%, the elongation at break decreased from 7.07% to 6.38% and the tensile strength increased to 71.06 MPa, corresponding to an increase of approximately 27% relative to the pure PLA. However, when fiber content increased further to 2%, the tensile property of the MCC/PLA composite sheet did not show further improvement. This may be due to the uneven distribution of MCC.

Unlike MCC, the APS-modified cellulose did not endow the AMCC/PLA composite with enhanced tensile property, as manifested by a larger reduction in both elongation at break and the modulus, and a smaller increase in the tensile strength relative to PLA. This unexpected result may be due to the reduced aspect ratio of the modified cellulose. In addition, the smoother surface of AMCC is not conducive to preventing pull-out from the PLA matrix.

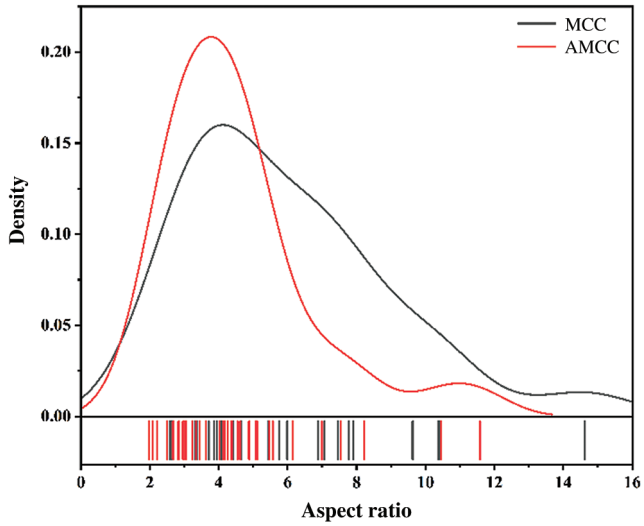

Figure 2: Normal distribution of the cellulose aspect ratio before and after modification

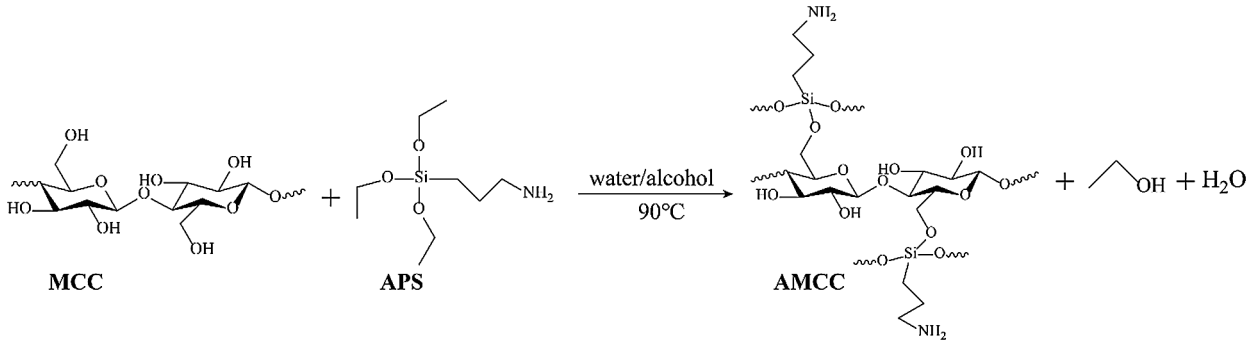

Scheme 1: APS-modified MCC

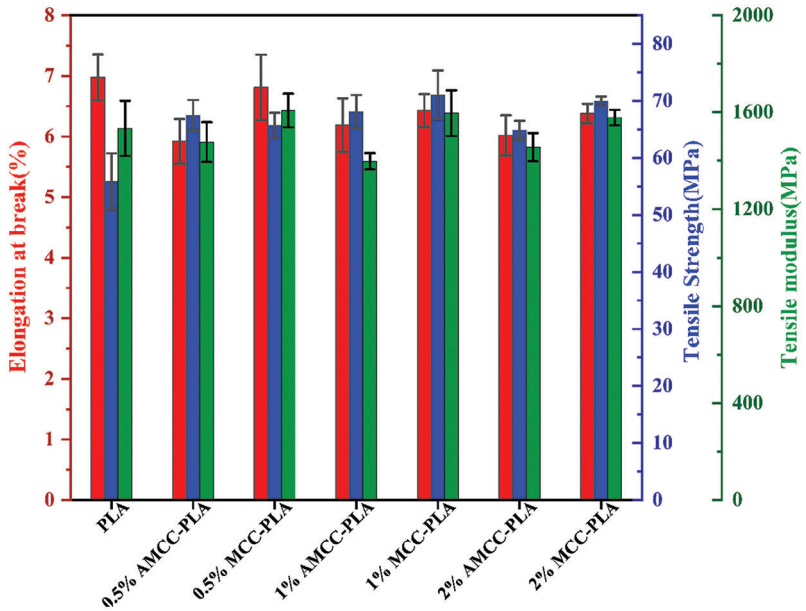

Figure 3: Elongation at break, tensile strength and tensile modulus of neat PLA and PLA/MCC composites

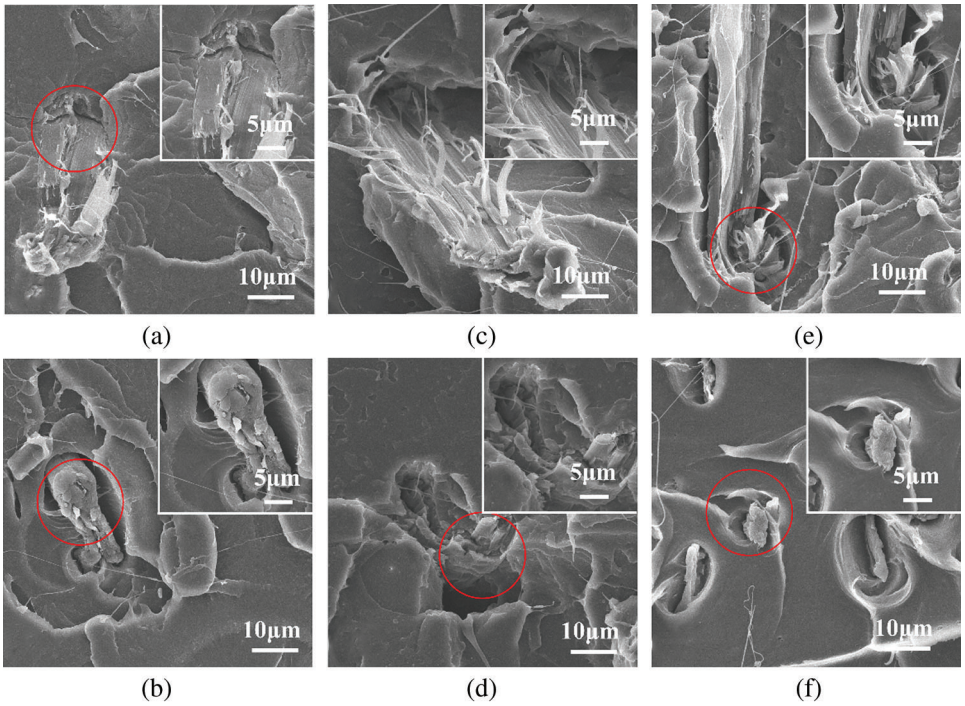

Figure 4: SEM of the fractured surfaces of AMCC-PLA composites: 0.5% (a), 1% (c), 2% (e); MCC-PLA composites: 0.5% (b), 1% (d), 2% (f)

4.3 Microstructure of PLA Composites

Figs. 4a, 4c and 4e show the cross-sections of the 0.5%, 1%, and 2% AMCC/PLA composite materials. APS undergoes hydrolysis and its methoxy functional group becomes a hydroxyl group, and then undergoes dehydration condensation reaction with cellulose, and the C-Si-O bond is formed on the cellulose. This reduces the hydroxyl groups on the surface of cellulose, so that the polarity of cellulose is reduced, and its compatibility with the polylactic acid matrix is improved. A smaller gap between the modified cellulose AMCC and PLA matrix is observed and the cellulose surface is torn. This shows that the strength of the bonding between the modified cellulose and the polylactic acid is greater than that of the hydrogen bond bonding among the modified cellulose molecules. Therefore, the fracture occurs on the modified cellulose.

Figs. 4b, 4d and 4f show the cross-sectional scanning electron micrographs of the PLA composite materials reinforced with unmodified cellulose (0.5%, 1%, 2%). The broken sections of the MCC/PLA composite show a weaker MCC-PLA connection compared to AMCC-PLA due to the incompatibility of cellulose and PLA. Together with the above-described analysis of mechanical properties (Fig. 2), these results indicate that the unmodified cellulose has a better reinforcement effect than the modified cellulose. This may be attributed to its rougher surface (Fig. 1b). The polylactic acid matrix ensures good contact between the surfaces by covering the rough cellulose surface, and prevents the fracture of the adhesive joint by dissipating energy under stress [38]. Thus, more energy is required to pull MCC out of the matrix. Even though the interface compatibility between AMCC and PLA is better than that between MCC and PLA, the former consumed less energy than MCC/PLA during breaking.

Generally, although the interface compatibility of the APS-modified cellulose has been further improved, the roughness of the fiber surface is reduced, and at the same time, the content of the fibers

with a high aspect ratio that exert a reinforcing effect is reduced. As a result, although modified cellulose has a certain enhancement effect, the enhancement effect is not as high as that for the unmodified cellulose.

4.4 DSC Analysis

Fig. 5 shows the DSC thermal analysis results for the neat PLA and its composites. The obtained glass transition temperature (T_g), cold crystallization temperature (T_{cc}), melting temperature (T_{m1}, T_{m2}), cold crystallization enthalpy (ΔH_{cc}), and melting enthalpy (ΔH_m) obtained by DSC are summarized in Tab. 1. In this study, the crystallinities of PLA and its composite materials are calculated as follows:

$$\chi_{sample}\% = (\Delta H_m - \Delta H_{cc})/\Delta H_m^0 \times 100\% \quad (2)$$

where ΔH_m^0 is the melting enthalpy of PLA for 100% crystallization and is 93.7 J/g.

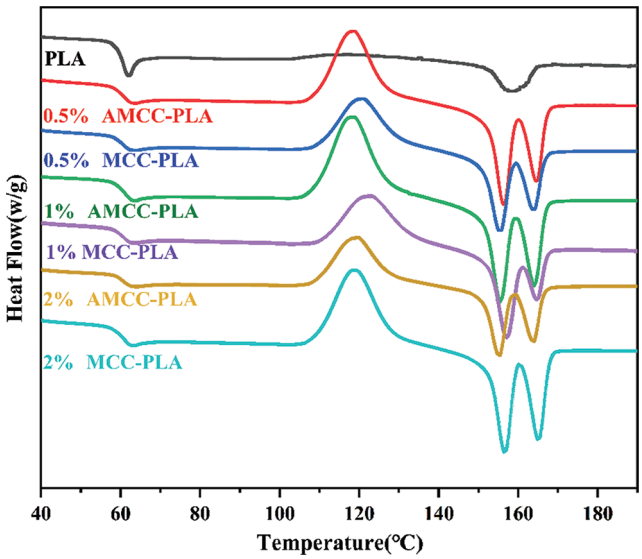

Figure 5: DSC thermograms of neat PLA, MCC/PLA composites: 2nd heating run

Table 1: DSC results for neat PLA and pulp fiber-reinforced PLA composites

Sample	T_g (°C)	T_{cc} (°C)	T_{m1} (°C)	T_{m2} (°C)	ΔH_{cc} (J/g)	ΔH_m (J/g)	X_{sample}% (%)
PLA	62.05	125.32	–	158.87	3.34	6.60	3.48
0.5% AMCC-PLA	63.43	118.40	156.51	165.10	20.31	20.67	0.38
0.5% MCC-PLA	62.92	120.52	155.23	163.61	16.33	17.62	1.38
1% AMCC-PLA	63.83	117.84	155.21	163.58	23.60	23.85	0.27
1% MCC-PLA	63.19	121.99	157.06	165.42	16.91	17.75	0.90
2% AMCC-PLA	63.43	118.77	154.97	164.00	14.30	14.81	0.54
2% MCC-PLA	62.93	118.76	156.27	165.16	21.93	23.89	2.09

With the addition of pulp cellulose, T_{cc} decreased due to the effect of heterogeneous nucleation. Pulp fiber plays a role of a heterogeneous nucleus in PLA and promotes the cold crystallization of the PLA

chains at lower temperatures. The neat PLA shows a single crystal melting peak, while its composite material shows a double melting peak (Fig. 5). This is because at a lower scan rate, there is sufficient time to melt the thinner crystal, and then reach the higher second melting peak. The addition of pulp fiber promotes recrystallization at higher temperatures. This indicates that MCC promotes the crystallization of PLA, including cold crystallization and recrystallization. Even though in the present study, the overall crystallinity of PLA did not show an increase upon the addition of cellulose, the change in the peak indicates the presence of crystallization. The T_{m2} of the composites is much higher than that of PLA, which is beneficial for improving the mechanical properties of the MAF-reinforced PLA at high temperature.

An examination of the DSC curves shows that both neat PLA and its composites have a crystallization peak at approximately 120°C. For polymer composites, the change in T_g is caused by the physical or chemical change that constrains the polymer chain. This is usually caused by the interaction between the polymer matrix and cellulose. Compared to neat PLA, the T_g of the MCC/PLA composites increased by approximately 0.43–0.93°C, indicating the absence of a significant interaction between the PLA matrix and the fiber.

4.5 DMA Analysis

As shown in Fig. 6a, compared to neat PLA, the storage modulus (E′) of the composite increases by approximately 50% or higher at 30°C. For both unmodified and modified cellulose, with increasing cellulose content, the E′ of the resulting composite rose. Compared to the unmodified cellulose, the increase obtained using modified cellulose is lower at the same concentration, which is similar to the results for the mechanical properties. The addition of cellulose limited the mobility of the polymer chain, leading to a rapid E′ drop for the neat PLA and its composites at nearly 50°C. For reinforced composites, E′ rose slightly at 105°C and then declined due to the obvious cold crystallization. Compared to the modified cellulose composites, the composites with unmodified cellulose present higher E′ values. This is because that the unmodified cellulose has a higher aspect ratio and rougher surface, necessitating higher energy input to separate it from the matrix.

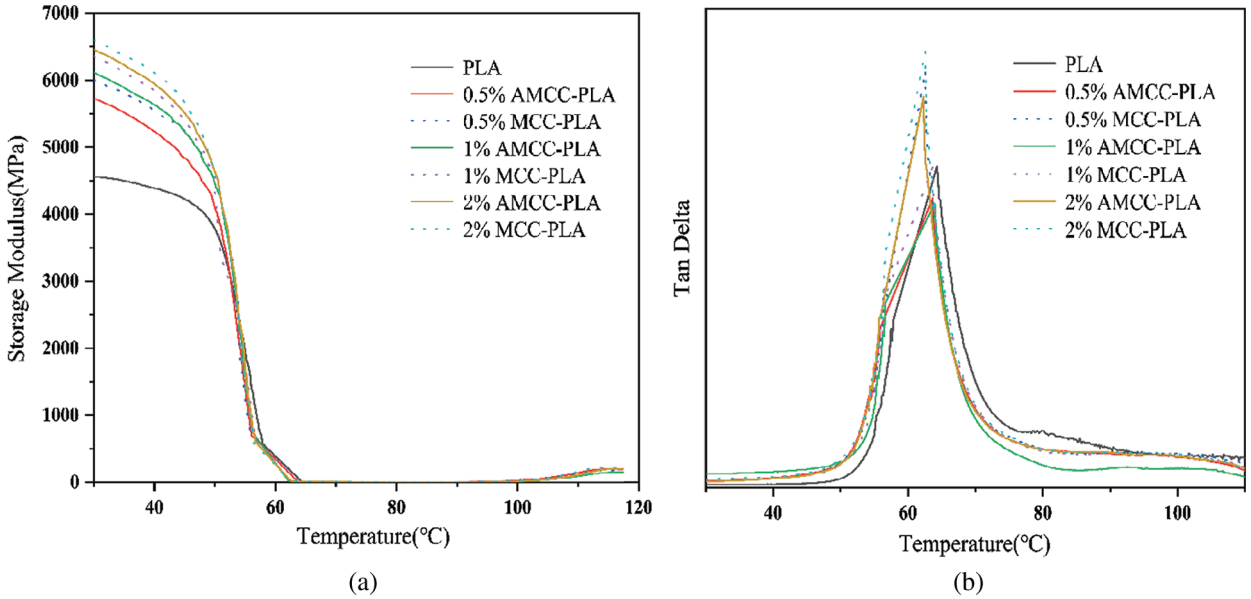

Figure 6: Dynamic mechanical analysis of neat PLA and pulp/PLA composites: (a) storage modulus, (b) tan(δ)

The tan(δ) curves **(**Fig. 6b**)** show that due to the addition of cellulose, the composite material presents a sharper and more intense peak than the neat PLA, except for the composite obtained with the addition of 2% AMCC. This indicates that the loss modulus of cellulose-reinforced PLA had a larger proportion of viscoelasticity in the composites than PLA. Thus, the composites obtained in this work did not present a great decrease in toughness unlike the other composites reported in the literature [39].

4.6 TGA and DTG Analysis

Fig. 7 shows the TGA and DTG test curves of pure PLA and its composite materials. Compared to PLA, the cellulose-reinforced composites thermally degraded at a relative lower temperature, albeit at a lower rate (Fig. 7b). With the increase in the cellulose content, the maximum degradation temperature of the composite materials did not evidently decrease. The lowest maximum degradation temperature of the composites is 354°C, which is 6°C lower than that for pure PLA. A similar phenomenon was reported in a previous study [26]. The decrease in the lowest maximum degradation temperature is due to the lower initial degradation temperature of the MCC that leads to decreased thermal stability of the composite upon MCC addition. The TG results for AMCC are similar to those for MCC, indicating that APS modification did not change the thermal behavior relative to MCC.

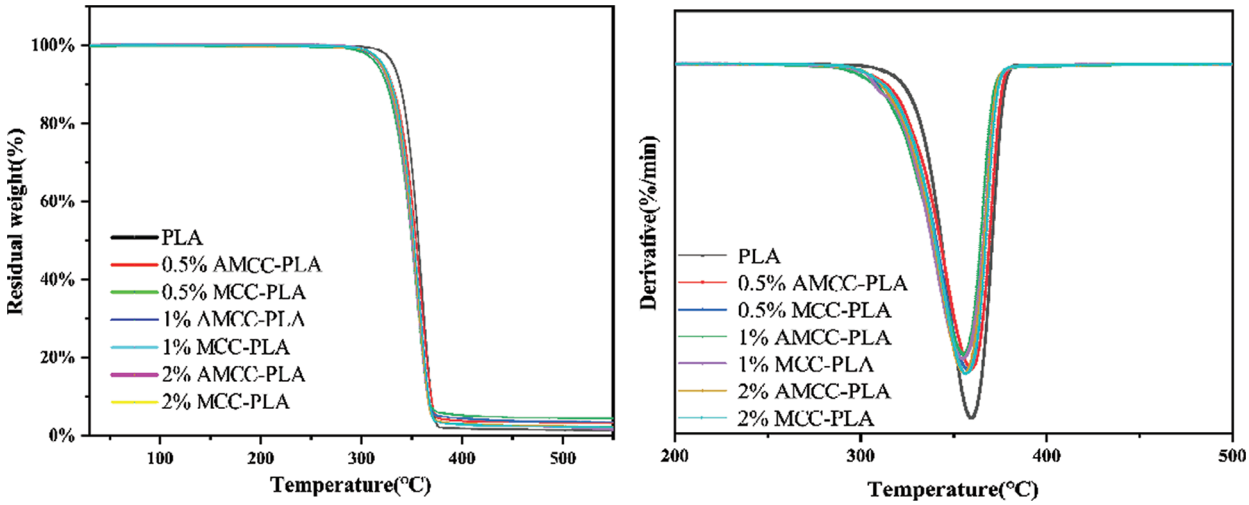

(a) (b)

Figure 7: Thermal stability of neat PLA and PLA/MCC composites: (a) TGA and (b) DTG curves

4.7 Transparency Analysis

Fig. 8a shows the transparency test results of polylactic acid and its composite materials. When the PLA sheet is placed on the school badge, the effect of the film is essentially negligible, demonstrating that the neat PLA shows the best transparency among the samples. Fig. 8b shows the photograph of the 2% unmodified cellulose reinforced PLA composite film. When it is spread on the black table, the black background is almost invisible. When it is placed on the school badge, the school badge can be seen (Fig. 8f), indicating that the obtained composite film exhibits a certain haze.

The result obtained using the UV spectrophotometer (Fig. 8g) shows that the transmittance of pure PLA reached 90% and then the transmittance was reduced to 40% upon addition of 0.5% unmodified cellulose. When the unmodified cellulose content increased to 2%, the transmittance of the composite film further decreased to approximately 20%. This is due to the bifurcation of the cellulose filaments and their non-uniform distribution in the PLA matrix.

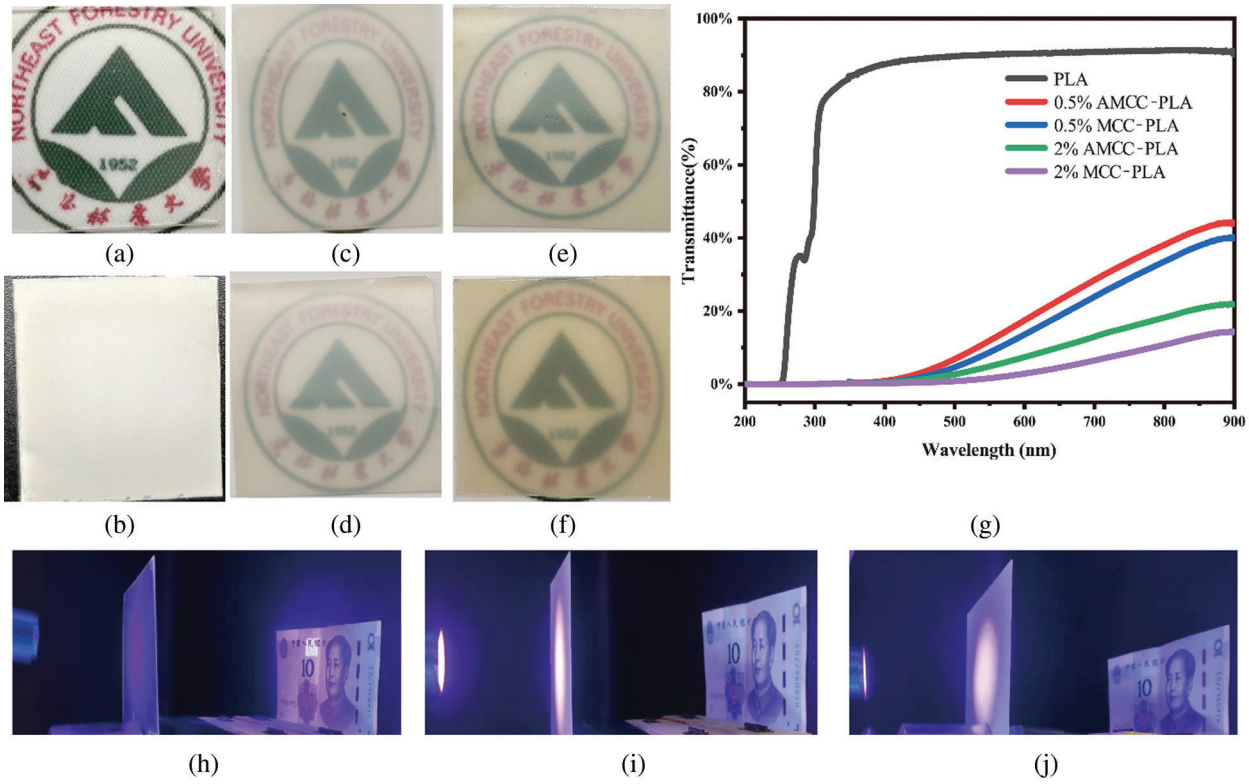

Figure 8: Digital images of (a) neat PLA, (b) 2% MCC/PLA in black background, (c) 0.5% and (d) 2% AMCC/PLA in crest, (e) 0.5% and (f) 2% MCC/PLA in crest; (g) UV spectrophotometer test results; (h) neat PLA and (i) 1% MCC/PLA (j) 2% MCC/PLA composite film under a UV lamp

When the modified cellulose was added, the transmittance of the AMCC/PLA composite films was higher compared to that of the composites with the unmodified cellulose. This is because that the APS modification treatment improved the uniformity of cellulose distribution and thus increased light transmittance. Figs. 8h–8j show the fluorescence of the films. When 300 nm ultraviolet light passes through the neat PLA film, the fluorescent watermark of RMB appeared clearly (Fig. 8h**)**. By contrast, when the ultraviolet light was transmitted through the 1% MCC/PLA and 2% MCC/PLA composite film, the UV color correspondent reaction on the RMB watermark is not observed **(**Fig. 8i). This is attributed to the network-like cellulose structure formed in PLA with the gap between the cellulose nets absorbing ultraviolet light, so that no fluorescence color reaction on the RMB characters occurred.

5 Conclusion

In the present study, a deep eutectic solvent was used to treat the pulp fibers and strongly reduce the size of the cellulose fibers. The cellulose was mixed with PLA by the solution mixing method to improve its distribution uniformity. The composites were successfully prepared by melt-blending and hot-pressing. Due to the presence of cellulose (0.5%–1%), the tensile strength and tensile modulus of the polylactic acid composite materials were significantly improved while the elongation at break of the neat PLA was retained. Contrary to expectation, the APS-modified cellulose did not provide better reinforcement than the unmodified cellulose. Both the thermal stability and the total crystallinity of polylactic acid decreased upon the addition of cellulose. It is concluded that the rougher surface and larger aspect ratio of MCC give rise to the improved tensile property and storage modulus. The cellulose-reinforced PLA composite

film shows a certain degree of transmittance, and the APS-modified fiber presents better transmittance due to its more uniform distribution. The combination of a deep eutectic solvent treatment and solution mixing is an effective method for the preparation of high-performance cellulose-reinforced PLA composites.

Funding Statement: This research was supported by the Natural Science Foundation of China (No. 32071704).

Conflicts of Interest: The authors declare that they have no conflicts of interest to report regarding the present study.

References

1. Lule, Z., Kim, J. (2019). Thermally conductive and highly rigid polylactic acid (PLA) hybrid composite filled with surface treated alumina/nano-sized aluminum nitride. *Composites Part A: Applied Science and Manufacturing, 124,* 105506. DOI 10.1016/j.compositesa.2019.105506.
2. Hashima, K., Nishitsuji, S., Inoue, T. (2010). Structure-properties of super-tough PLA alloy with excellent heat resistance. *Polymer, 51(17),* 3934–3939. DOI 10.1016/j.polymer.2010.06.045.
3. Manzanares Palenzuela, C. L., Novotný F., Krupička, P., Sofer, Z., Pumera, M. (2018). 3D-printed graphene/polylactic acid electrodes promise high sensitivity in electroanalysis. *Analytical Chemistry,* 90(9), pp. 5753–5757. DOI 10.1021/acs.analchem.8b00083.
4. França, D. C., Almeida, T. G., Abels, G., Canedo, E. L., Carvalho, L. H. et al. (2019). Tailoring PBAT/PLA/Babassu films for suitability of agriculture mulch application. *Journal of Natural Fibers, 16(7),* 933–943. DOI 10.1080/15440478.2018.1441092.
5. Arrieta, M. P., López, J., Ferrándiz, S., Peltzer, M. A. (2013). Characterization of PLA-limonene blends for food packaging applications. *Polymer Testing, 32(4),* 760–768. DOI 10.1016/j.polymertesting.2013.03.016.
6. Jo, M. Y., Ryu, Y. J., Ko, J. H., Yoon, J. S. (2012). Effects of compatibilizers on the mechanical properties of ABS/PLA composites. *Journal of Applied Polymer Science, 125(S2),* E231–E238. DOI 10.1002/app.36732.
7. Murariu, M., Dubois, P. (2016). PLA composites: From production to properties. *Advanced Drug Delivery Reviews, 107,* 17–46. DOI 10.1016/j.addr.2016.04.003.
8. Claro, P. I. C., Neto, A. R. S., Bibbo, A. C. C., Mattoso, L. H. C., Bastos, M. S. R. et al. (2016). Biodegradable blends with potential use in packaging: A comparison of PLA/chitosan and PLA/cellulose acetate films. *Journal of Polymers and the Environment, 24(4),* 363–371. DOI 10.1007/s10924-016-0785-4.
9. Silva, C. G., Campini, P. A., Rocha, D. B., Rosa, D. S. (2019). The influence of treated eucalyptus microfibers on the properties of PLA biocomposites. *Composites Science and Technology, 179,* 54–62. DOI 10.1016/j.compscitech.2019.04.010.
10. Frone, A. N., Berlioz, S., Chailan, J. F., Panaitescu, D. M. (2013). Morphology and thermal properties of PLA–cellulose nanofibers composites. *Carbohydrate Polymers, 91(1),* 377–384. DOI 10.1016/j.carbpol.2012.08.054.
11. Ambrosio-Martín, J., Fabra, M. J., Lopez-Rubio, A., Lagaron, J. M. (2015). Melt polycondensation to improve the dispersion of bacterial cellulose into polylactide via melt compounding: Enhanced barrier and mechanical properties. *Cellulose, 22(2),* 1201–1226. DOI 10.1007/s10570-014-0523-9.
12. Chen, W., Yu, H., Liu, Y., Chen, P., Zhang, M. et al. (2011). Individualization of cellulose nanofibers from wood using high-intensity ultrasonication combined with chemical pretreatments. *Carbohydrate Polymers, 83(4),* 1804–1811. DOI 10.1016/j.carbpol.2010.10.040.
13. Frone, A. N., Berlioz, S., Chailan, J. F., Panaitescu, D. M. (2013). Morphology and thermal properties of PLA–cellulose nanofibers composites. *Carbohydrate Polymers, 91(1),* 377–384. DOI 10.1016/j.carbpol.2012.08.054.
14. Yang, Z., Li, X., Si, J., Cui, Z., Peng, K. (2019). Morphological, mechanical and thermal properties of poly(lactic acid)(PLA)/cellulose nanofibrils (CNF) composites nanofiber for tissue engineering. *Journal of Wuhan University of Technology-Materials Science Edition, 34(1),* 207–215. DOI 10.1007/s11595-019-2037-7.

15. Hassan, M. M., Le Guen, M. J., Tucker, N., Parker, K. (2019). Thermo-mechanical, morphological and water absorption properties of thermoplastic starch/cellulose composite foams reinforced with PLA. *Cellulose, 26(7),* 4463–4478. DOI 10.1007/s10570-019-02393-1.
16. Chen, J. C., Lin, J. C. (2018). Manufacturing and properties of cotton and jute fabrics reinforced epoxy and PLA composites. *International Journal of Modern Physics B, 32(19),* 1840084. DOI 10.1142/S0217979218400842.
17. Zhang, X., Ding, W., Chang, E., Chen, X., Chen, J. et al. (2020). Foaming behaviors and mechanical properties of injection-molded polylactide/Cotton-fiber composites. *Industrial & Engineering Chemistry Research, 59(40),* 17885–17893. DOI 10.1021/acs.iecr.0c03348.
18. Mazzanti, V., Pariante, R., Bonanno, A., de Ballesteros, O. R., Mollica, F. et al. (2019). Reinforcing mechanisms of natural fibers in green composites: Role of fibers morphology in a PLA/hemp model system. *Composites Science and Technology, 180,* 51–59. DOI 10.1016/j.compscitech.2019.05.015.
19. Pappu, A., Pickering, K. L., Thakur, V. K. (2019). Manufacturing and characterization of sustainable hybrid composites using sisal and hemp fibres as reinforcement of poly(lactic acid) via injection moulding. *Industrial Crops and Products, 137,* 260–269. DOI 10.1016/j.indcrop.2019.05.040.
20. Porras, A., Maranon, A. (2012). Development and characterization of a laminate composite material from polylactic acid (PLA) and woven bamboo fabric. *Composites Part B: Engineering, 43(7),* 2782–2788. DOI 10.1016/j.compositesb.2012.04.039.
21. Zhang, L., Lv, S., Sun, C., Wan, L., Tan, H. et al. (2017). Effect of MAH-g-pLA on the properties of wood fiber/polylactic acid composites. *Polymers, 9(11),* 591. DOI 10.3390/polym9110591.
22. Mukherjee, T., Tobin, M. J., Puskar, L., Sani, M. A., Kao, N. et al. (2017). Chemically imaging the interaction of acetylated nanocrystalline cellulose (NCC) with a polylactic acid (PLA) polymer matrix. *Cellulose, 24(4),* 1717–1729. DOI 10.1007/s10570-017-1217-x.
23. Pirani, S., Abushammala, H. M., Hashaikeh, R. (2013). Preparation and characterization of electrospun PLA/nanocrystalline cellulose-based composites. *Journal of Applied Polymer Science, 130(5),* 3345–3354. DOI 10.1002/app.39576.
24. Xian, X., Wang, X., Zhu, Y., Guo, Y., Tian, Y. (2018). Effects of MCC content on the structure and performance of PLA/MCC biocomposites. *Journal of Polymers and the Environment, 26(8),* 3484–3492. DOI 10.1007/s10924-018-1226-3.
25. Wang, X., Tang, Y., Zhu, X., Zhou, Y., Hong, X. (2020). Preparation and characterization of polylactic acid/polyaniline/nanocrystalline cellulose nanocomposite films. *International Journal of Biological Macromolecules, 146,* 1069–1075. DOI 10.1016/j.ijbiomac.2019.09.233.
26. He, L., Song, F., Li, D. F., Zhao, X., Wang, X. L. et al. (2020). Strong and tough polylactic acid based composites enabled by simultaneous reinforcement and interfacial compatibilization of microfibrillated cellulose. ACS *Sustainable Chemistry & Engineering, 8(3),* 1573–1582. DOI 10.1021/acssuschemeng.9b06308.
27. Qian, S., Zhang, H., Yao, W., Sheng, K. (2018). Effects of bamboo cellulose nanowhisker content on the morphology, crystallization, mechanical, and thermal properties of PLA matrix biocomposites. *Composites Part B: Engineering, 133,* 203–209. DOI 10.1016/j.compositesb.2017.09.040.
28. Spinella, S., Re, G. L., Liu, B., Dorgan, J., Habibi, Y. et al. (2015). Polylactide/cellulose nanocrystal nanocomposites: Efficient routes for nanofiber modification and effects of nanofiber chemistry on PLA reinforcement. *Polymer, 65,* 9–17. DOI 10.1016/j.polymer.2015.02.048.
29. Wang, X., Tang, Y., Zhu, X., Zhou, Y., Hong, X. (2020). Preparation and characterization of polylactic acid/polyaniline/nanocrystalline cellulose nanocomposite films. *International Journal of Biological Macromolecules, 146,* 1069–1075. DOI 10.1016/j.ijbiomac.2019.09.233.
30. Zhang, Q., Lei, H., Cai, H., Han, X., Lin, X. et al. (2020). Improvement on the properties of microcrystalline cellulose/polylactic acid composites by using activated biochar. *Journal of Cleaner Production, 252,* 119898. DOI 10.1016/j.jclepro.2019.119898.
31. Li, P., Sirviö, J. A., Haapala, A., Liimatainen, H. (2017). Cellulose nanofibrils from nonderivatizing urea-based deep eutectic solvent pretreatments. ACS *Applied Materials & Interfaces, 9(3),* 2846–2855. DOI 10.1021/acsami.6b13625.

32. Ma, Y., Xia, Q., Liu, Y., Chen, W., Liu, S. et al. (2019). Production of nanocellulose using hydrated deep eutectic solvent combined with ultrasonic treatment. ACS *Omega, 4(5),* 8539–8547. DOI 10.1021/acsomega.9b00519.
33. Smith, E. L., Abbott, A. P., Ryder, K. S. (2014). Deep eutectic solvents (DESs) and their applications. *Chemical Reviews, 114(21),* 11060–11082. DOI 10.1021/cr300162p.
34. Espino, M., de los Ángeles Fernández, M., Gomez, F. J., Silva, M. F. (2016). Natural designer solvents for greening analytical chemistry. *TrAC Trends in Analytical Chemistry, 76,* 126–136. DOI 10.1016/j.trac.2015.11.006.
35. Murphy, C. A., Collins, M. N. (2018). Microcrystalline cellulose reinforced polylactic acid biocomposite filaments for 3D printing. *Polymer Composites, 39(4),* 1311–1320. DOI 10.1002/pc.24069.
36. Lin, N., Huang, J., Chang, P. R., Feng, J., Yu, J. (2011). Surface acetylation of cellulose nanocrystal and its reinforcing function in poly(lactic acid). *Carbohydrate Polymers, 83(4),* 1834–1842. DOI 10.1016/j.carbpol.2010.10.047.
37. Nam, S., French, A. D., Condon, B. D., Concha, M. (2016). Segal crystallinity index revisited by the simulation of X-ray diffraction patterns of cotton cellulose Iβ and cellulose II. *Carbohydrate Polymers, 135,* 1–9. DOI 10.1016/j.carbpol.2015.08.035.
38. Rose, S., Prevoteau, A., Elzière, P., Hourdet, D., Marcellan, A. et al. (2014). Nanoparticle solutions as adhesives for gels and biological tissues. *Nature, 505(7483),* 382–385. DOI 10.1038/nature12806.
39. Du, Y., Wu, T., Yan, N., Kortschot, M. T., Farnood, R. (2014). Fabrication and characterization of fully biodegradable natural fiber-reinforced poly(lactic acid) composites. *Composites Part B: Engineering, 56,* 717–723. DOI 10.1016/j.compositesb.2013.09.012.